A precision, low-cost vibrating sample magnetometer

*A. Niazi, P. Poddar and A. K. Rastogi**

A high quality, low-cost vibrating sample magnetometer (VSM) for the study of magnetic properties of materials in high magnetic fields in the temperature range 80–350 K has been constructed. An important feature of the VSM is a stable electrodynamic vibrator electronically controlled using feedback and error minimization. The vibrator, associated electronics and liq-N_2 flow cryostat have been made using locally available low-cost materials in a modest budget of a few thousand rupees. The VSM incorporates ease of sample change, good sensitivity for magnetic moment measurements and precise temperature control and its measurement. Test and calibration have been done using standard samples and the performance compares very well with extremely costly imported systems. The VSM is suitable for teaching laboratories as well as specialized research work involving measurements of weak magnetic moments of small quantities of samples.

THE study of magnetic properties of materials is a basic requirement for understanding electronic behaviour in condensed matter. Many varieties of inorganic compounds and alloys of transition metals have been synthesized wherein the electrons show highly correlated behaviour; i.e. the conduction electrons depend on the presence or absence of neighbouring electrons. These electronic correlations result in magnetism, superconductivity, metal–insulator transitions or heavy-fermion behaviour of conduction electrons. These different types of behaviour depend upon the strength of Coulomb and exchange interactions among electrons. The study of these interactions among electrons requires magnetic measurement at low temperatures and high magnetic fields.

Many types of magnetometers have been developed and are now commercially available. They have been extensively reviewed by Foner[1,2] and can be broadly classified into two categories: (i) Those employing direct techniques, such as measurement of the force experienced by the specimen in a non-uniform field (Guoy, Faraday, Kahn balances); (ii) Those based on indirect techniques such as measurement of magnetic induction due to relative motion between the sample and the detection coils system (vibrating sample, vibrating coil, SQUIDs) or use of galvanomagnetic effects such as the Hall effect. The vibrating sample magnetometer (VSM) developed originally by Foner[2], has however, been the most successful for low temperature and high magnetic field studies of correlated electron systems due to its simplicity, ruggedness, ease of measurement and reasonably high sensitivity.

Working principle of VSM

The VSM is based upon Faraday's law according to which an *e.m.f.* is induced in a conductor by a time-varying magnetic flux. In VSM, a sample magnetized by a homogenous magnetic field is vibrated sinusoidally at a small fixed amplitude with respect to stationary pick-up coils (Figure 1). The resulting field change $\partial\mathbf{B}(t)$ at a point $\mathbf{r}$ inside the detection coils induces voltage and is given by

$$V(t) = \sum_n \int_A \frac{\partial \mathbf{B}(t)}{\partial t} \cdot \mathrm{d}\mathbf{A}, \tag{1}$$

where $\mathbf{A}$ is the area vector of a single turn of the coil and the summing is done over n turns of the coils. $\mathbf{B}(t)$ is given by the dipolar approximation, assuming small dimensions of the magnetized sample in comparison to its distance from the detection coils,

$$\mathbf{B}(\mathbf{r}) = \frac{\mu_0}{4\pi}\left(\frac{\mathbf{m}}{r^3} - \frac{3(\mathbf{m}\cdot\mathbf{r})\mathbf{r}}{r^3}\right), \tag{2}$$

and

$$\frac{\partial B_i(t)}{\partial t} = \frac{\partial \mathbf{a}(t)}{\partial t} \cdot \vec{\nabla}_{\mathrm{r}} \{B(r)\}_i, \tag{3}$$

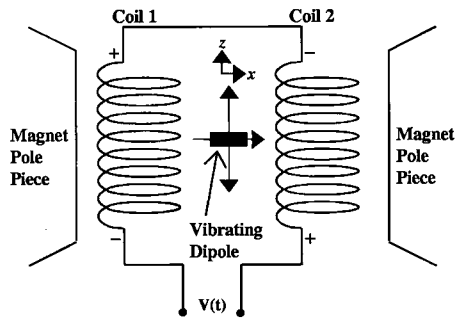

Figure 1. Working principle of VSM.

The authors are in the School of Physical Sciences, Jawaharlal Nehru University, New Delhi 110 067, India
*For correspondence. (e-mail: rastogi@jnuniv.ernet.in)

$\mathbf{a}(t)$ being the position of the dipole and $\{B(r)\}_i$, $i = 1, 2, 3$, the ith component of **B** at **r** due to dipole **m**. $V(t)$ can be detected to a high resolution and accuracy by means of suitable associated electronics. For stationary pick-up coils and a uniform and stable external field, the only effect measured by the coils is that due to the motion of the sample. The voltage $V(t)$ is thus a measure of the magnetic moment of the sample.

Design and construction details

Our VSM consists of the following subsystems: Electromagnet and power supply; sample vibrator with associated electronic circuit; detection coils; signal recovery using lock-in-amplifier; cryostat and sample holder.

In the following sections we shall discuss each subsystem in detail.

Electromagnet and power supply

An extremely stable and homogenous magnetic field is required in order to achieve maximum sensitivity of the VSM. Any field instability or external vibrations of coils placed in a non-homogenous field would be picked up by the detection coils, thus reducing the sensitivity of magnetization measurement.

A Laboratory Electromagnet model 3473–70 from M/S GMW Associates, USA with the following specifications is used for the magnetizing field:

- Pole diameter: 6″; pole gap: 0–3.8″; pole caps: 2″ tapered.
- Maximum power to coils (water cooled): 70 A/59 V (4.1 kW).
- Field at 2″ pole face and 1 ″pole gap: 1.7 Tesla at 70 A.

A high stability low noise constant current output power supply Model 858 System 8000 from M/S Danfysik A/S, Jyllinge, Denmark is used to generate the magnetizing field. This power supply gives 5 ppm load regulation and 0.05 ppm/°C temperature coefficient for the magnetizing current. It features an inbuilt IEEE-GPIB interface for control using a PC. A locally procured Hall probe-based Gaussmeter is used to measure the field.

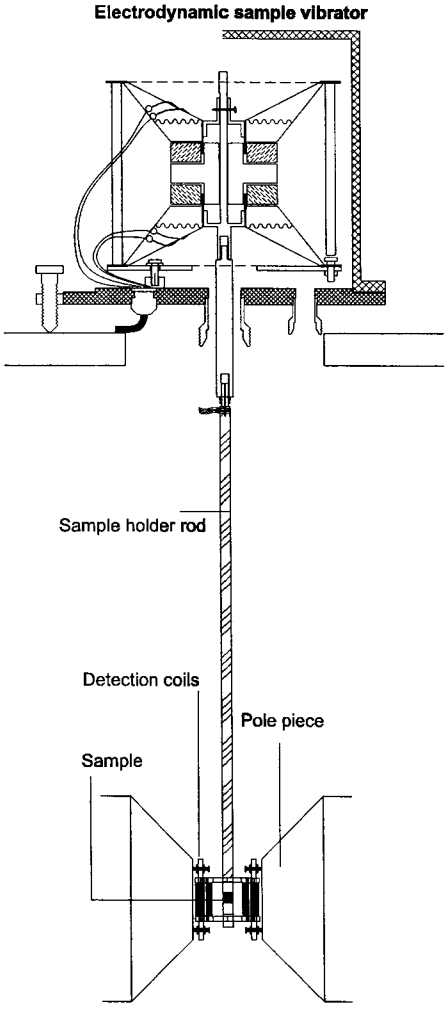

Figure 2. Schematic of VSM showing the overall assembly.

Sample vibrator and associated electronic circuit

The hallmark of VSM (Figure 2) is an in-house designed and constructed sample vibrator (Figure 3), built to fulfill the following principal requirements: (i) Pure sinusoidal vibrations of constant frequency; (ii) Stability of vibration amplitude under load variation and friction; (iii) Stable reference signal phase for lock-in detection of the signal.

Electrodynamic vibrator: We have used two Bolton™ mid-range audio speakers (30 W/8Ω, 12 cm cone) available from the local market. The ferrite ring magnets were demagnetized and carefully detached from the speakers.

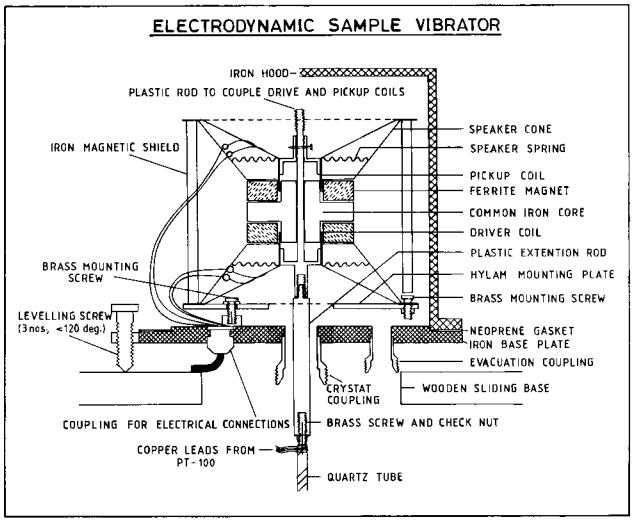

Figure 3. Schematic of the electrodynamic sample vibrator.

The individual central iron cores were replaced by a single specially machined soft-iron core having a central bore. The ferrite cores were then glued using epoxy on either face of the common core, and remagnetized. The speaker cone and coil sections were then glued to their respective ferrite cores so that the two speakers were mounted back-to-back (Figure 3). The vibrating coils of the speakers were coupled to each other by a 5 mm diameter plastic (Metalon^{TM}) rod passing through the central bore within the iron core and glued to the speaker coils taking care that the coils could move freely within the small core gap. Both ends of the coupling rod were threaded for attaching the sample rod. The back-to-back coupled speakers were then mounted on an iron baseplate. It is necessary that the vibrations of the coil during its operation are not transferred to the base plate and thence to the cryostat and detection coils. Hence antivibration mountings were used. A suitable levelling arrangement consisting of three levelling screws was also incorporated on the iron base plate.

In this arrangement, one of the coils of the vibrator is used as a drive coil for sample vibration while the other acts as a velocity-sensing coil. The signal from the sensing coil is used for negative feedback in order to achieve better stability of sample vibrations.

Electronic circuit: An elaborate electronic circuit has been designed for controlling the above vibrator. It was constructed using locally available components. The block diagram of the electronic circuit is shown in Figure 4. The circuit incorporates the following features:

- A sine-wave generator with 20–170 Hz variable frequency adjustment.
- Reference signal (2 V rms) for phase-sensitive detection.
- Maximum amplitude adjustment.
- Gain and bandwidth adjustment of the feedback loop.
- Facility for error minimization between required and actual driver amplitude and frequency.

The error minimization facility is a variable voltage feed which can be applied directly to the power amplifier. This has an in-phase (proportional) component and also a phase-lagging (integral) component with respect to the reference voltage (chosen velocity). In this way a substantial reduction in the difference (error) between the required velocity and that obtained through the sensing coil of the driver can be achieved. This feature is essential in order to operate the driver coil very near to the reference velocity irrespective of variations in load and frictional changes in the vibrator and sample support. This allows one to calibrate the magnetometer at a fixed reference velocity using standard samples of known magnetization. The same vibration conditions can then be used for the magnetization measurements of unknown samples.

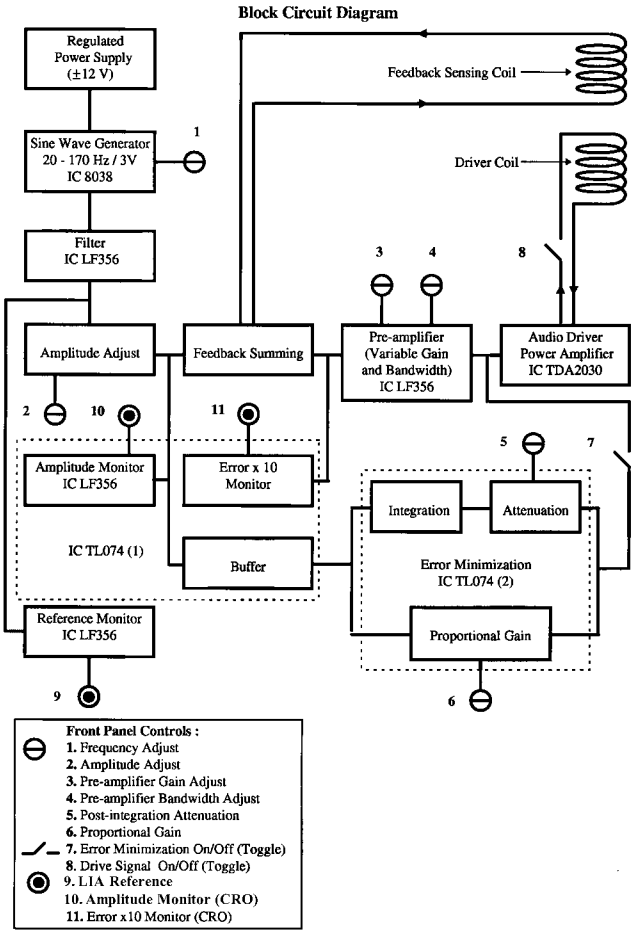

Figure 4. Block diagram for the electronic circuit used to control the sample vibrator. The details of each block are presented in the Appendix.

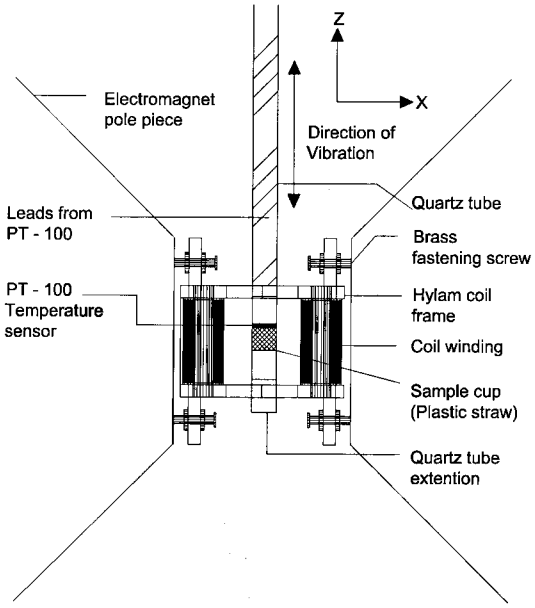

Figure 5. Geometry for the vibration axis, sample position, detection coils and applied magnetic field.

Detailed circuit diagrams for each block in Figure 4 are given in the Appendix.

Detection coils

In order to measure **m** by eq. (1), various geometries of detection coils as well as the direction of vibration-axis of the sample with respect to magnetizing field direction are possible – single or a set of multi-detection coils arranged with axes parallel or perpendicular to the field direction. For example, when using the solenoidal magnetic fields of a superconducting magnet, the axes of detection coils and sample vibration are parallel to **m**. However, this geometry is inconvenient for conventional iron-core electromagnets as it requires special modifications to the pole faces. It is also extremely vulnerable to small magnetic field inhomogeneities and sample position. The following general considerations therefore determine the optimal coil arrangements for any set-up:

- Proper compensation of pick-up coils to minimize effects of noise from external magnetic disturbance.
- A broad saddle point whereby the signal is immune to small changes in the mean position of the sample.
- Optimization of dipole flux linkage with coils in order to maximize signal-to-noise (Johnson noise) ratio.
- Sufficient space for cryostat tail in the smallest possible pole gap.
- Ease of sample change and alignment of the sample-rod.

We have chosen for our electromagnet (max. field of 1.7 T in a 40 mm pole gap) the geometry for vibration axis, detection coils and field as shown in Figure 5. The sample is at the origin (centre of the pole gap) and vibrates along the z-axis while the magnetic field and the associated sample moment are along the x-axis. We use a pair of compensated Foner coils[1] placed equidistant from the sample with axes parallel to the z-axis. The coils are arranged so that any variation in the external magnetic flux induces voltage in a series opposing sense at their terminal. For this requirement, the coils are placed (Figure 1), symmetrically about the x–y and x–z planes but anti-symmetrically about the y–z plane, i.e. viewing along the z-axis both have the same sense of winding. This geometry makes the magnetization measurements insensitive to small changes in the sample position and mechanical vibrations in the magnet, as well as magnetic flux changes from any source away from the coils.

Signal pick-up is as follows: The dipole oscillates along the z-axis with amplitude $a(t) = a \sin(wt)$. As the dipole moves upward (+ ve z direction), by Lenz's law the net axial component of $\mathbf{B}(\mathbf{r})$ through coil 1 increases in the downward direction, while in coil 2 it increases in the upward direction. Since the coil turns are in the same direction, the combined e.m.f.s of the two coils add up at the terminal to give a net signal free of external noise. The voltage induced in the pick-up coils is given by eq. (1)

$$V(t) = \frac{3}{4\pi} m\mu_0 \omega \cos(wt) a$$

$$\sum_n \int_A \frac{\mathrm{d}A}{r^7} \cdot \{z(r^2 - 5x^2)\hat{i} - 5xyz\,\hat{j} + x(r^2 - 5z^2)\hat{k}\}. \quad (4)$$

The symmetry of the coils about the x–z and x–y planes results in the terms odd in y or z integrating to zero-induced voltage. Only the kth component terms of the induced voltage remain. This coil arrangement has been referred to as the kth detection system by Bowden[4].

Optimization of the detection coil system: Bowden[4] has calculated equi-value contours of the function $g_k(r, \theta, \phi = 0)$ corresponding to the kth component of eq. (4),

$$g_k(r, \theta, \phi) = \frac{x(r^2 - 5z^2)}{r^7} = \frac{\sin\theta(1 - 5\cos^2\theta)}{r^4}. \quad (5)$$

It is found that there is a restriction on the coil height vs position since the signal changes sign at $\theta = 63.43°$, where θ is the angular position of the coil w.r.t. the origin.

In accordance with the above dimensional restrictions, our coils are layer wound using 0.112 mm copper wire

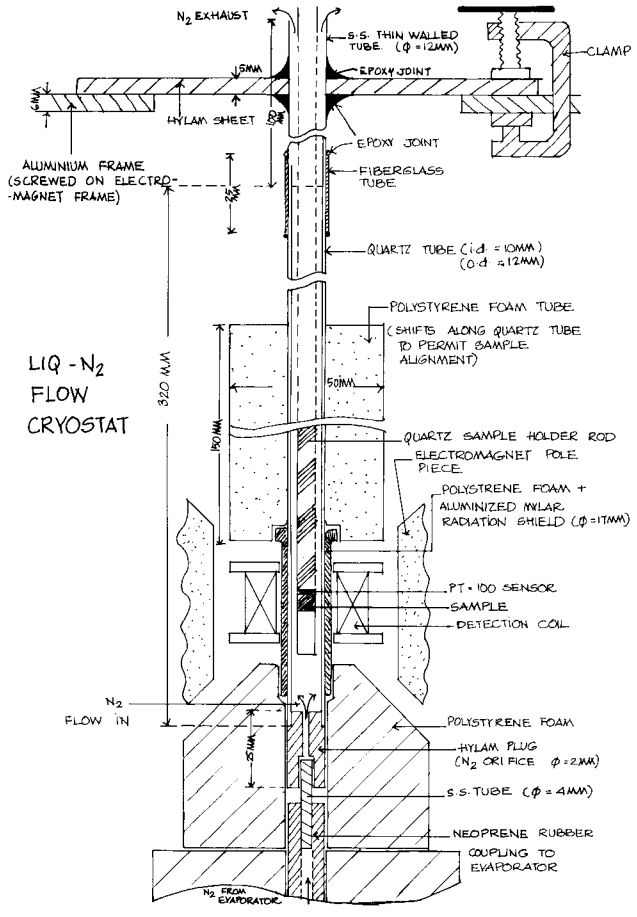

Figure 6. Schematic of liq-N_2 flow cryostat.

on Hylam^{TM} bobbins (length = 20 mm, i.d. = 5 mm, o.d = 10 mm). 2800 turns per coil gave a resistance of 97Ω at 300 K. The coils are mounted in a non-magnetic Hylam^{TM} frame with coil centre-to-centre distance of 28 mm and central bore of 17.5 mm. The coil assembly is securely jacked between the pole faces in a 40 mm pole gap.

Signal recovery using lock-in-amplifier

Weakly paramagnetic systems produce very small signals in the detection coils. Special processing of the pick-up signals is required to filter out random noise and achieve high sensitivity of the magnetometer. We can estimate the size of the pick-up signal for a typical paramagnet having $\chi \approx 10^{-6}$ emu/cc and volume ≈ 0.1 cc placed in a 10^4 Gauss magnetic field.

In CGS units: $\chi = 10^{-6}$, $B = 10^4$ G, magnetization density $M = \chi B = 10^{-2}$ emu/cc, magnetic moment $m = 10^{-3}$ emu.

In SI units: $\chi = 4\pi 10^{-6}$, $B = 1$ T, $M_{SI} = (4\pi 10^{-6}/\mu_0)$ A/m, magnetic moment $m = 10^{-6}$ A m^{-2}.

An estimate of the amplitude of the signals expected in our system can be obtained by considering a pair of flat coils with 100 turns each placed at $x = \pm 14 \times 10^{-3}$ m and $y = z = 0$, connected in series addition. The sample with **m** in the x direction is vibrated along the z-axis with frequency $f = 80$ Hz and amplitude $a = \pm 1 \times 10^{-3}$ m. Using the kth component from eq. (5), amplitude part of the signal is given by

$$V = \frac{6}{\pi} m\mu_0 \omega a \sum_n \int_A \frac{dA}{r^7} \cdot \{x(r^2 - 5z^2)\hat{k}\}. \quad (6)$$

We obtain $V_0 \approx 250$ nV (peak), or V_0 $(rms) \approx 175$ nV. Thus, for our chosen geometry and coil dimensions, signals of 100 nV–1 μV are expected. It is obvious that in order to achieve a resolution ≤ 1% of the signals, lock-in (phase-sensitive) detection of the signals and a large rejection of common mode noise is necessary. However, for experiments on magnetic specimen, a laboratory-made phase sensitive detector such as a four-diode-bridge sampling gate followed by a d.c. amplifier may be sufficient.

We have used a lock-in-amplifier (LIA) model no. SR530 (Stanford Reseach Systems, USA) connected to the detection coils in differential input mode. The LIA has 100 dB CMRR and when operated under low dynamic reserve it has 5 ppm/°C stability. For operation at 80 Hz reference frequency using bandwidth as well as line (50 Hz) filters, a pre-filter time constant of 3 sec and post-filter time constant of 1 sec gave the maximum noise reduction.

In the course of testing of the magnetometer, it was found that small coherent signals (~ 100 nV) from the magnetic fields of the vibrator coils and from the current leads of the driver can directly couple to the detection coils. Proper positioning of the driver current leads and shielding of the vibrator assembly by a mild-steel hood is essential to eliminate this spurious coherent signal.

For correct measurements of magnetic moments, the reference phase for the LIA can be properly adjusted

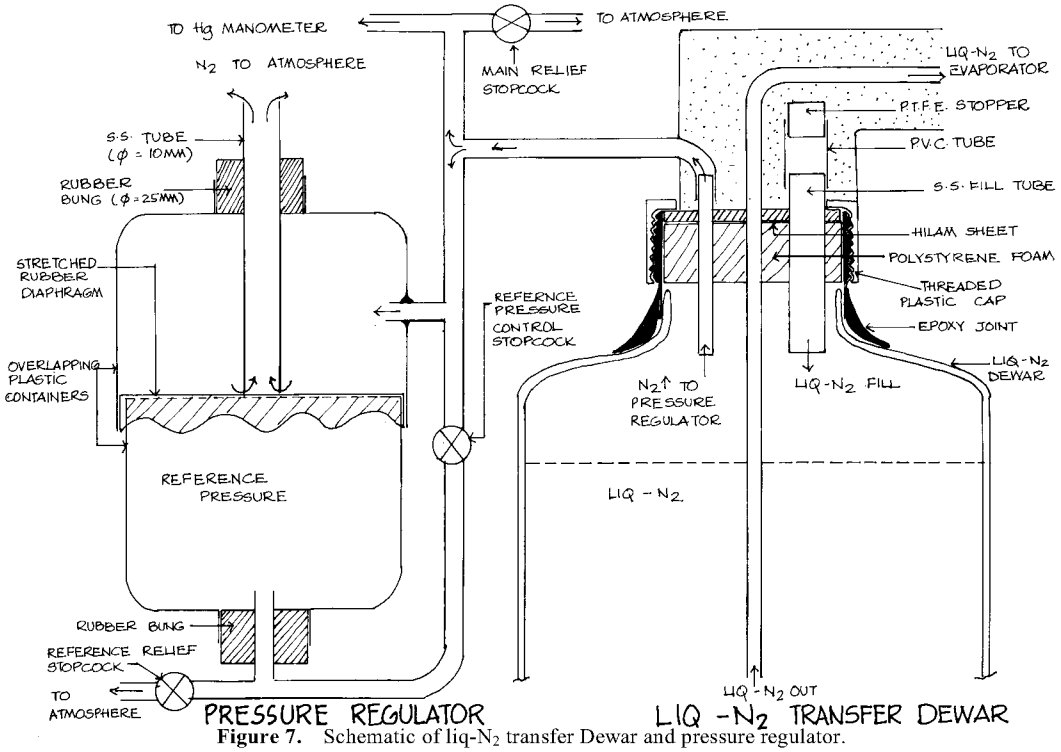

Figure 7. Schematic of liq-N_2 transfer Dewar and pressure regulator.

using a large in-phase signal from a sample of paramagnetic salt such as $CuSO_4 \cdot 5H_2O$ or $MnCl_2 \cdot 4H_2O$. The detailed results of calibration of the magnetometer using various standard samples are presented in a later section.

Cryostat and sample holder

The sample holder rod and cryostat have been built keeping in mind the following general design requirements:

- The sample holder rod should permit easy coupling/decoupling from the vibrator to facilitate sample change.
- The holder rod should be light, non-magnetic and mechanically rigid throughout the temperature range.
- The detection coils are situated outside the cryostat. Therefore there should be no signal attenuation, i.e. the cryostat tail should be made of non-metallic and non-magnetic materials.
- The sample holder rod should be perfectly aligned along the cryostat axis so that it vibrates freely. Since minor adjustments are required every time a sample is replaced, the cryostat should permit inspection of the sample rod alignment.
- The cryostat should be isolated from the sample vibrations transmitted through the vibrator mounting plate.
- The temperature in the cryostat should be precisely controlled. For a flow cryostat, that means efficient regulation of pressure, i.e. flow and temperature of the coolant gas.
- The sample temperature should be accurately monitored using a non-magnetic sensor.

Cryostat: Our flow-cryostat (Figure 6) is constructed using 10 mm i.d. quartz tubing properly insulated by a sheath of polystyrene foam. The foam can be shifted up so that the transparent cryostat tail permits easy sample alignment. The upper end of the quartz tube is coupled to a non-magnetic s.s. tube which is in turn fixed with epoxy to a Hylam^{TM} sheet firmly clamped to the electromagnet frame. A pressure regulator (Figure 7) using a rubber sheet diaphragm valve and mercury manometer is connected to the liq-N_2 storage dewar and maintains constant coolant flow. The coolant, under 5–7 cm Hg pressure, passes through an evaporator (Figure 8) before reaching the sample. The evaporator consists of a 3 mm Cu tubing coiled around a 12 mm Cu rod and sunk using Pb–Sn solder. A Cu-constantan thermocouple monitors the temperature of the gas while a 30 Ω heater wrapped around the coils provides 50 W of heater power. The evaporator is encased in Hylam^{TM} tubing with an insulating polystyrene foam sheath. We use a PID-based temperature controller model no. ITC-4 (Oxford Instruments Ltd, UK) to regulate the coolant temperature.

Sample holder: The sample holder rod (Figure 2, overall view) is made of a quartz tubing (6 mm o.d.) as quartz has the lowest coefficient of thermal contraction and can be repeatedly cycled down to 80 K without fracturing. A brass screw fixed with epoxy to one end couples it to the vibrator rod. A calibrated miniature PT-100 temperature sensor (2 × 5 mm) glued to the other end stays in intimate contact with the sample cup. Bi-filially wound 41 BSW Cu leads from the PRT are drawn along the rod and taken out from the top end. The PRT is an ideal sensor for use in magnetic fields down to 30 K and sample temperature

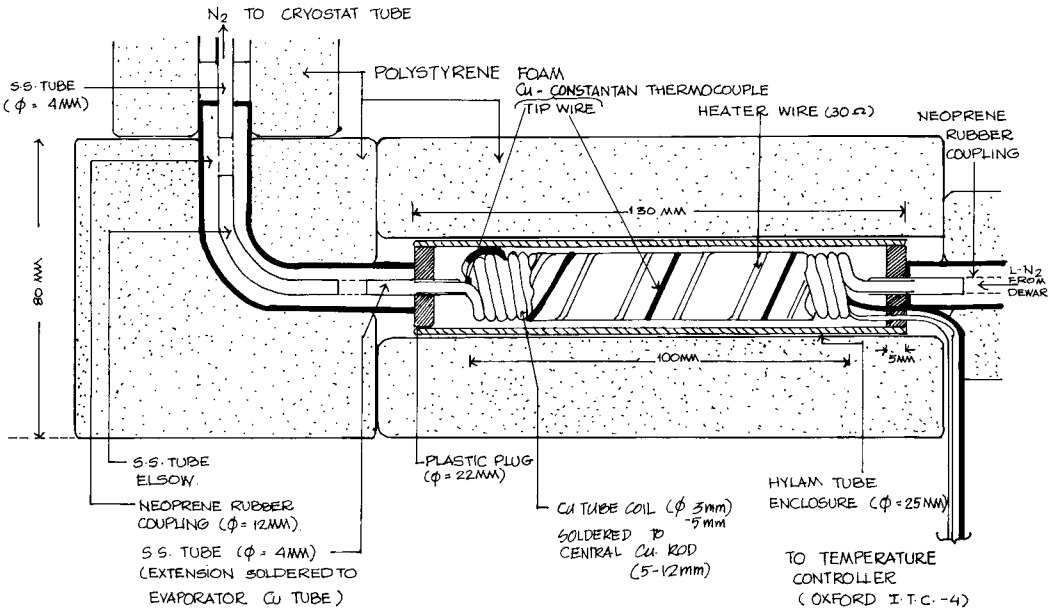

Figure 8. Schematic of liq-N_2 evaporator.

is accurately monitored by 4-wire measurements using a Keithley 195 DMM.

The sample cup (Figure 5, detailed view) consists of a piece of ordinary plastic drinking straw of 6 mm diameter to fit snugly over the holder rod. A 5 mm length in the centre contains the tightly packed sample powder with paper plugs on either side. Cu wire is coiled outside and glued using varnish (General Electric) to thermally sink the sample. A 15 mm stub of quartz tube attached to the bottom of the sample cup is also required to cancel the small signal from the upper portion of the quartz sample holder rod.

Magnetometer calibration

The voltage induced in the detection coils is a function of many variables including the finite dimensions of the coils and the sample, as well as the geometrical arrangement of the coil assembly vs sample. Thus, it is not possible to exactly calculate the integral of eq. (6) to obtain numerical values for the signal voltage. While the contour plots of eq. (5) are useful in coil design and placement to obtain a broad saddle point for the sample position[4], the final calibration of the set-up is done using standard samples with known magnetic properties. During calibration it is necessary to ensure that:

- Small changes in sample position and deviation from ideal spherical symmetry do not affect the calibration constant.
- The frequency and amplitude of vibrations stay constant.
- The sample holder, etc. contribute only small constant values to the signal which can be subtracted from the total signal.
- The signal voltage is a linear function of the sample magnetic moment.

A detailed study of the magnetometer sensitivity w.r.t. the sample position using coil parameters similar to ours has been carried out by Bowden[4]. It was found that a displacement of the mean position of sample by ± 1 mm from the centre along the x, y and z directions produced respectively 0.05%, 1% and 1% changes. The effect of deviation of sample geometry from the ideal spherical shape has been studied by Zieba and Foner[5] by considering the spherical harmonics expansion of a sensitivity function analogous to eq. (5). For a sample in the form of a right circular cylinder, of length-to-diameter ratio $\sim\sqrt{3}/2$, the first non-zero error term occurs only in the fourth-order, thus ensuring a flat response around the mean position.

In our case the space and limitation of the cryostat do not allow more than ± 1 mm displacement in the x and y directions. The z-axis positioning is done by the screw on the sample holder rod. The use of a quartz sample holder rod minimizes effects of thermal contraction with temperature variation. In Figure 9 we present the voltage signal from a magnetized Ni cylinder (4 mm diameter, 4 mm height) as its position is shifted along the z direction. We note that within ± 3.5 mm of displacement of sample position along the z-axis the observed voltage stays within ~ 5%. Our normal sample size is a cylinder of 6 mm diameter and 5 mm length. Therefore, using a standard paramagnetic salt sample for calibration, the inaccuracy of the estimated magnetization will be within 1–2%.

Measurement procedure

Samples of known mass are taken in powder form and tightly packed into the sample holder cup as described earlier. The vibrator frequency is kept around 79 Hz to minimize interference from 50 Hz a.c.-line noise. The amplitude adjust is 205 mV. The room-temperature magnetization is measured while varying the field from 0–1.5 T. For the M(T) measurements, at a constant applied field the temperature is swept between 80 and 350 K in approximately 3 h under a maintaining pressure of ~ 5–7 mm Hg. The pick-up voltage induced in the detection coils is fed to the LIA in differential mode. The sample temperature is monitored by a PT-100 sensor mounted next to the sample as described earlier. The data acquisition for the LIA as well as the sample temperature is done through IEEE-GPIB using in-house developed programmes.

The magnetic susceptibilty is calculated using the above calibration constant, C.C. as follows:

$$\chi\ (\text{emu/mole}) = V_{\text{signal}} \times \frac{\text{Formula wt.}}{\text{Wt. of sample}} \times \frac{\text{C.C.}}{H_{\text{applied}}}. \quad (7)$$

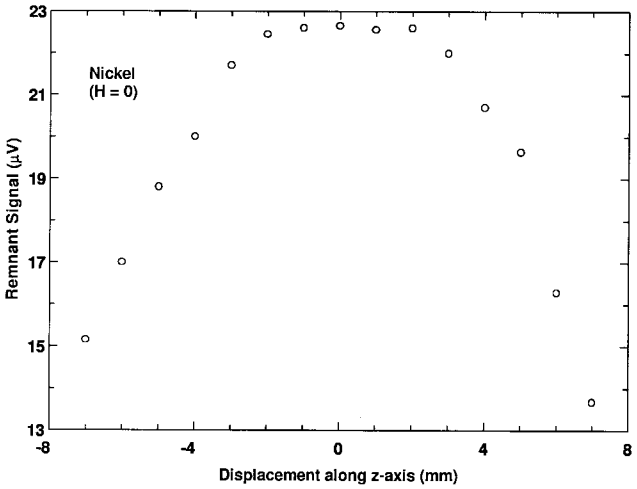

Figure 9. Remnant magnetization vs displacement along z-axis for Ni cylinder. Large flat region around zero shows that magnetization errors are less than 5%.

Tests performed

The following tests were done using standard samples:

- Linearity of signal w.r.t magnetic moment, for $CuSO_4 \cdot 5H_2O$ (Figure 10).
- Determination of C.C. using room-temperature saturation magnetization of ferromagnetic Ni (Figure 11) and Curie law obeying transition metal salt $CuSO_4 \cdot 5H_2O$ (Figure 12).
- Accuracy of temperature measurement from 80–350 K using the paramagnetic salt $CuSO_4 \cdot 5H_2O$ (Figure 12).

The C.C. was determined in two ways: (i) At room temperature using the saturation magnetization signal of Ni (Figure 11); (ii) From the slope of the $(\text{signal/mass})^{-1}$ vs T curve of $CuSO_4 \cdot 5H_2O$ (Figure 12). We find that the C.C. determined through two different ways is nearly the same. An average value of the two gives C.C. = 2×10^4 emu/V, which compares quite favourably with commercial set-ups[6].

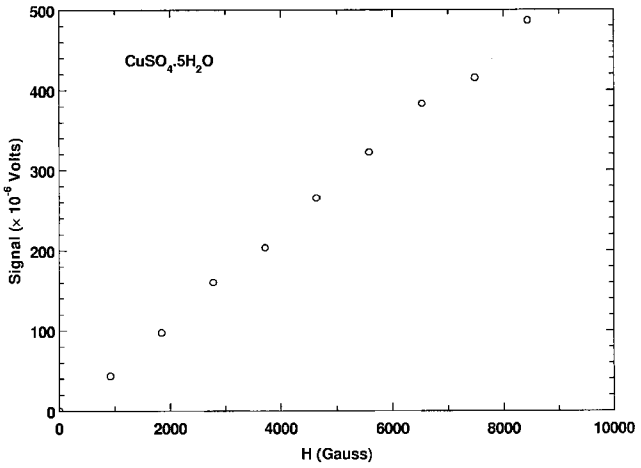

Figure 10. $M(H)$ curve at room temperature for $CuSO_4.5H_2O$ showing linearity of signal with applied field.

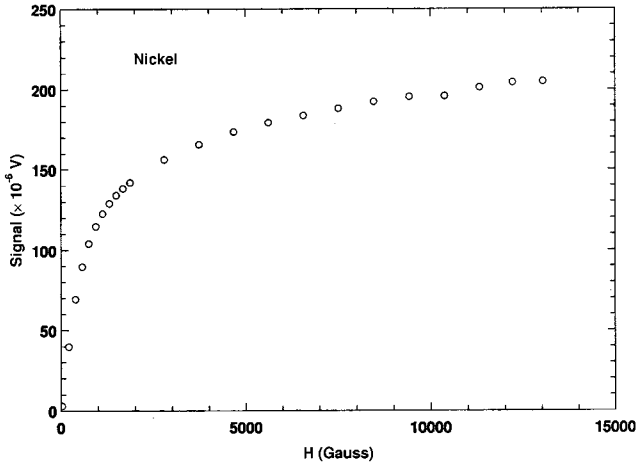

Figure 11. $M(H)$ curve at room temperature for nickel showing saturation magnetization.

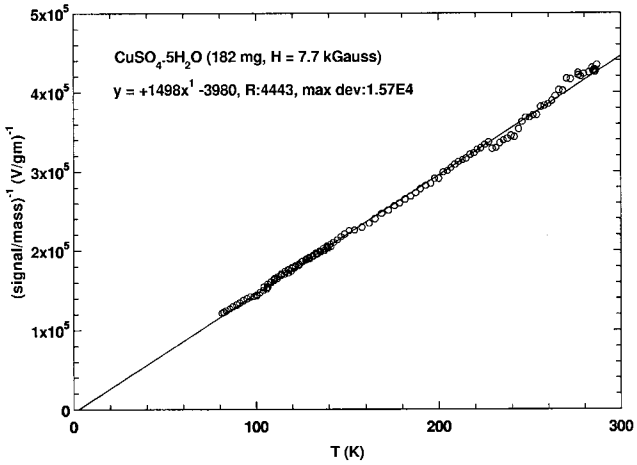

Figure 12. Magnetization^{-1} vs temperature plot of $CuSO_4.5H_2O$.

Potential use in teaching laboratories

In our VSM the costly electromagnet and LIA for signal recovery are used because of the special nature of our research work involving weakly magnetic materials. A large variety of materials showing magnetic, spin-glass or superconducting transitions as well as the study of Meissner effect or hysteresis in magnetic materials give order-of-magnitude larger signals[7]. The study of these interesting phenomena can be introduced in post-graduate teaching laboratories using an in-house available low-cost electromagnet and a.c.-amplifier. In view of their technological importance, study of these materials in teaching programmes is highly desirable. This low-cost VSM may provide a versatile tool for the above need.

Appendix

VSM circuit diagrams

Detailed circuit diagrams for the individual parts shown in the block diagram of the vibrator electronic circuit (Figure 4) are presented in the following order:

(1) Power supply (12–0–12 V, 2 A).
(2) Sine wave generator (20–170 Hz, 3 V_{rms}).
(3) Sine wave filter, attenuator, reference monitor.
(4) Error monitor, amplitude monitor and buffer (IC TL074(1)).
(5) Error minimization circuit (IC TL074(2)).
(6) Pre-amplifier and power-amplifier.

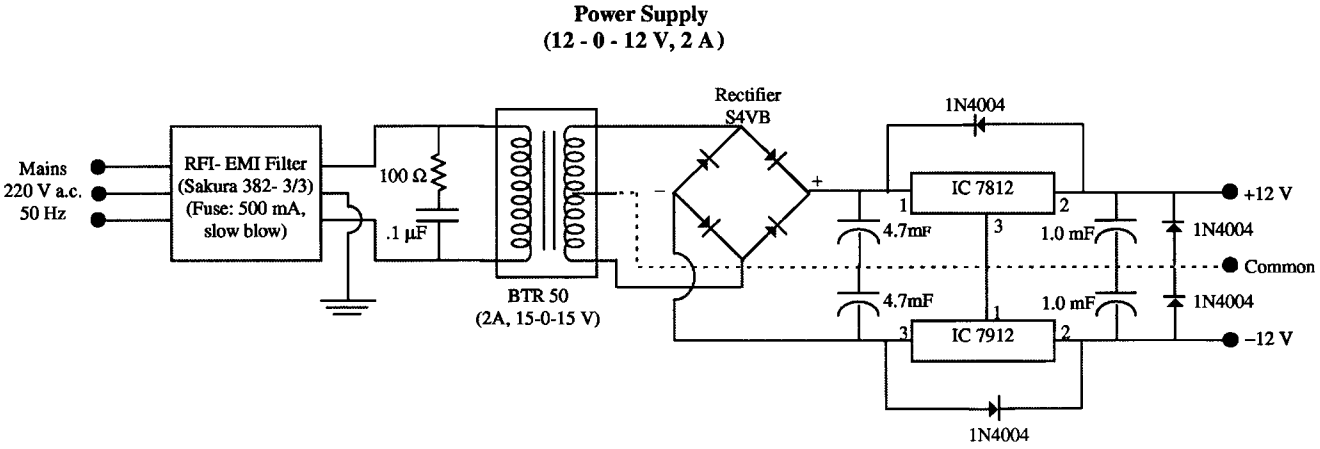

Circuit diagram 1.

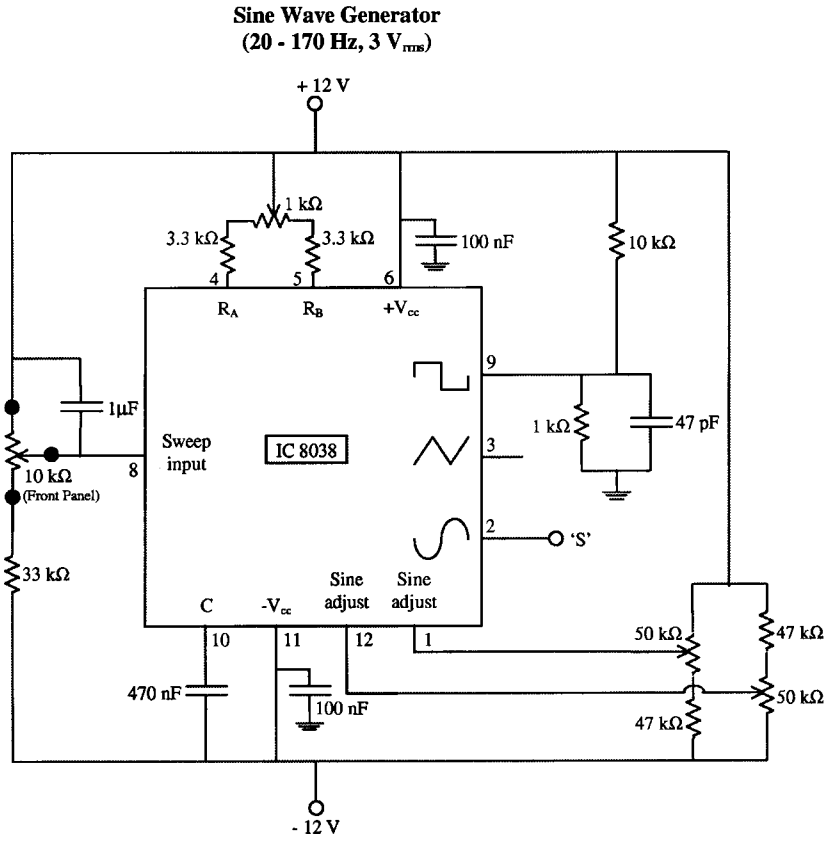

Circuit diagram 2.

Sine Wave Filter, Attenuator, Reference Monitor

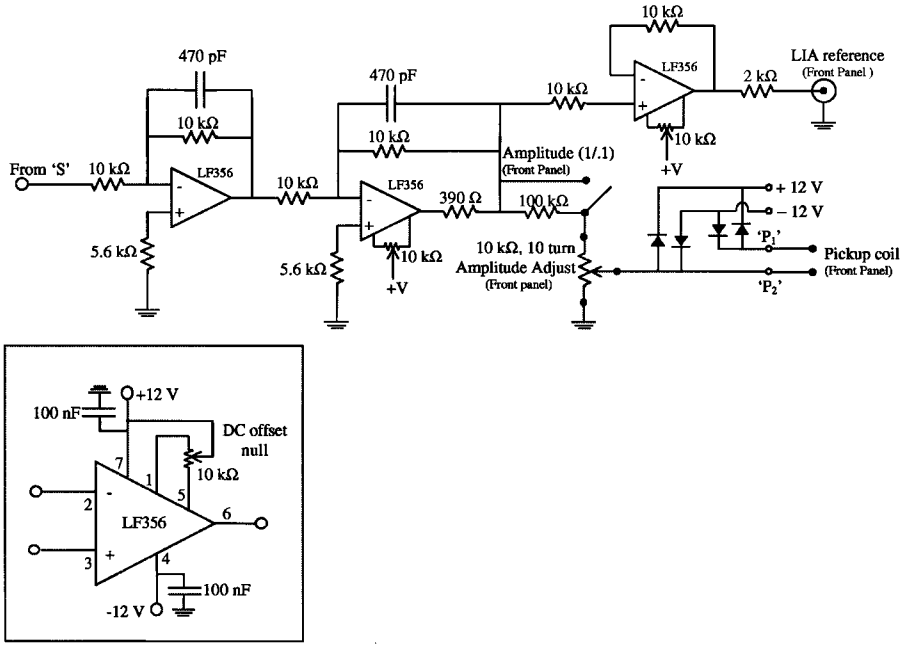

Circuit diagram 3.

Error Monitor, Amplitude Monitor and Buffer
IC TL074 (1)

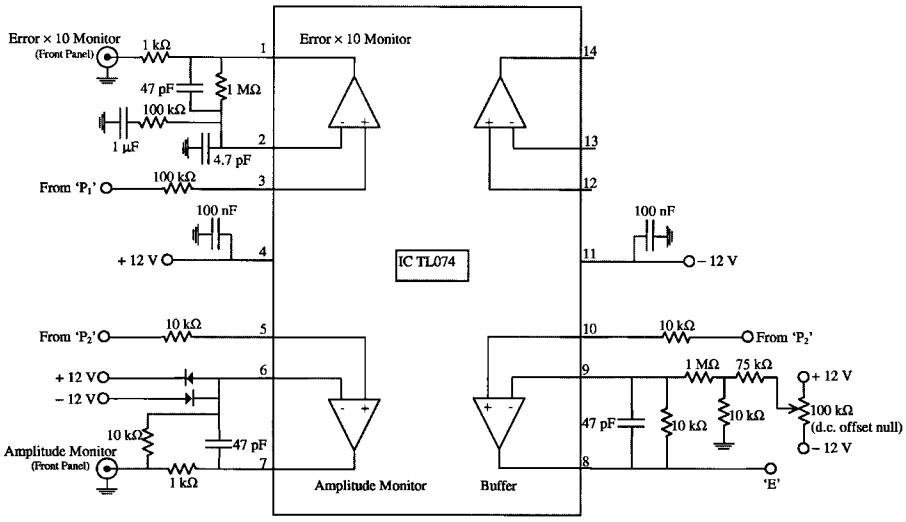

Circuit diagram 4.

Error Minimization Circuit
IC TL074 (2)

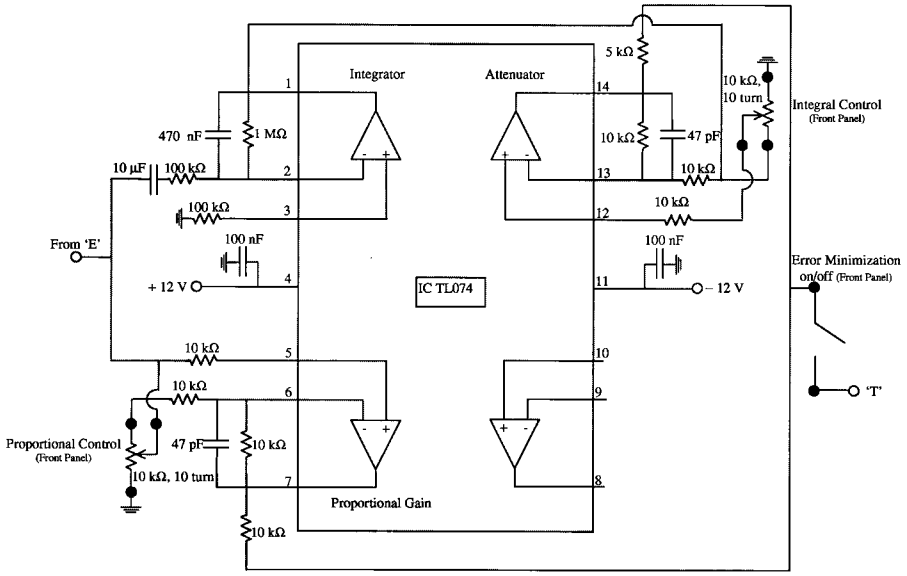

Circuit diagram 5.

Pre-Amplifier and Power-Amplifier

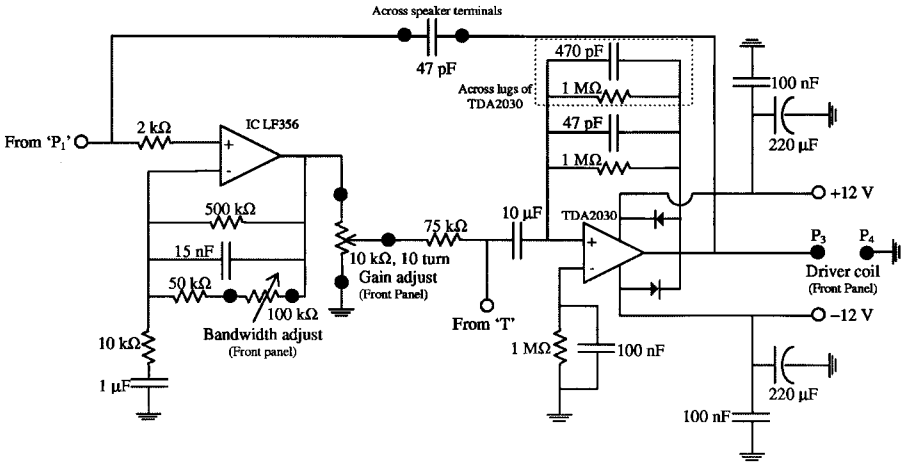

Circuit diagram 6.

1. Foner, S., *IEEE Trans. Magn.*, 1981, **17**, 3358–3363.
2. Foner, S., *J. Appl. Phys.*, 1996, **79**, 4740–4745.
3. Foner, S., *Rev. Sci. Instrum.*, 1959, **30**, 548–557.
4. Bowden, G. J., *J. Phys. E Sci. Instrum.*, 1972, **5**, 1115–1119.
5. Zieba, A. and Foner, S., *Rev. Sci. Instrum.*, 1982, **53**, 1344–1354.
6. The sensitivity of commercial VSMs depends on various noise reduction techniques. The LakeShore Model 7300 by Lake Shore Cryotronics Inc, USA has a noise level of 5×10^{-6} emu equivalent at the measurement time of 10 sec.
7. Kittel, C., *Introduction to Solid State Physics*, John Wiley, Singapore, 1995, 7th edn.

ACKNOWLEDGEMENTS. We thank M. S. Ruman for help in fabrication of the instrument. This work has been funded by SAP-DRS/1994-1999 grant of UGC, New Delhi. A.N. and P.P. acknowledge financial support from CSIR and UGC, New Delhi. Technical assistance from NSC, New Delhi in setting up the magnet is gratefully acknowledged.

Received 17 November 1999; revised accepted 3 April 2000